Spectral-Efficient Hybrid Dimming Scheme for Indoor Visible Light Communication: A Subcarrier Index Modulation Based Approach

Tengjiao Wang, *Student Member, IEEE*, Fang Yang, *Senior Member, IEEE*, Changyong Pan, *Senior Member, IEEE*, Ling Cheng, *Senior Member, IEEE*, and Jian Song, *Fellow, IEEE*

***Abstract*—Communication and illumination are two basic functions of the indoor visible light communication (VLC). In this paper, a novel spectral-efficient hybrid dimming scheme is proposed for the indoor VLC system, where the frequency-domain subcarrier selection is utilized to maximize the channel capacity and the intensity-domain dimming strategy is used to further adjust the illumination level. Simulations are carried out in both the indoor line-of-sight channel and the indoor multipath channel. Simulation results substantiate the superior performance of the proposed hybrid dimming scheme over the state-of-the-art schemes.**

***Index Terms*—Asymmetrically clipped optical OFDM, hybrid dimming control, line-of-sight channel, multipath channel, subcarrier index modulation, visible light communication.**

I. Introduction

IN RECENT years, the increasing demands of high-quality information services have posed challenging requirements for the future wireless communication systems [1]. Utilizing the unregulated visible light spectrum, visible light communication (VLC) has been recognized as a complementary technology to the conventional radio frequency communications [2].

Manuscript received March 11, 2019; revised June 1, 2019, July 31, 2019, and August 15, 2019; accepted August 26, 2019. Date of publication August 29, 2019; date of current version November 27, 2019. This work was supported in part by the National Natural Science Foundation of China under Grant 61871255, in part by the National Key Research and Development Program of China under Grant 2017YFE0113300, in part by the Natural Science Foundation of Guangdong Province under Grant 2015A030312006, in part by the Beijing National Research Center for Information Science and Technology Program under Grants BNR2019TD01001 and BNR2019RC01015, in part by the Tsinghua University Tutor Research Fund, and in part by South Africa's National Research Foundation (112248 & 114626). *(Corresponding author: Fang Yang.)*

T. Wang is with the Beijing National Research Center for Information Science and Technology (BNRist), Department of Electronic Engineering, Tsinghua University, Beijing 100084, China (e-mail: wangtj16@mails.tsinghua.edu.cn).

F. Yang, C. Pan, and J. Song are with the Beijing National Research Center for Information Science and Technology (BNRist), Department of Electronic Engineering, Tsinghua University, Beijing 100084, China, and also with the Key Laboratory of Digital TV System of Guangdong Province and Shenzhen City, Research Institute of Tsinghua University in Shenzhen, Shenzhen 518057, China (e-mail: fangyang@tsinghua.edu.cn; pcy@tsinghua.edu.cn; jsong@tsinghua.edu.cn).

L. Cheng is with the School of Electrical and Information Engineering, University of the Witwatersrand, Johannesburg 2000, South Africa (e-mail: ling.cheng@wits.ac.za).

Color versions of one or more of the figures in this article are available online at http://ieeexplore.ieee.org.

Digital Object Identifier 10.1109/JLT.2019.2938237

In VLC, orthogonal frequency-division multiplexing (OFDM) is widely adopted because of its inherent resilience to the inter-symbol interference (ISI) [3]. However, due to the physical characteristics of generating light in light-emitting diodes (LEDs), only the positive real intensity can be modulated to transmit information. Thus, the intensity modulation and direct detection (IM/DD) technology is generally considered in the VLC systems. So far, many kinds of OFDM based modulation methods have been proposed to generate the required positive real signals. In [4], a direct current adjustment based OFDM method, i.e. the direct current biased optical OFDM (DCO-OFDM), is proposed for the wireless infrared communication systems. This kind of modulation methods can be used in the VLC systems as well. In [5], the asymmetrically clipped optical OFDM (ACO-OFDM) is introduced to improve the energy efficiency. Using ACO-OFDM, the negative parts of the time-domain signals are clipped to generate positive real signals. However, in ACO-OFDM, only the odd subcarriers are modulated to transmit information bits, which causes a 3 dB/bit penalty in the spectral efficiency of the system. In order to improve the spectral efficiency, many hybrid OFDM methods have been further proposed [6], such as the asymmetrically clipped DC biased optical OFDM (ADO-OFDM) [7] and the layered OFDM methods. In ADO-OFDM, the system transmits ACO-OFDM signals on the odd subcarriers and DCO-OFDM signals on the even subcarriers simultaneously. The layered OFDM methods use superposition modulation to improve the spectral efficiency of the system, including the layered ACO-OFDM [8], the enhanced ACO-OFDM [9]–[11], the enhanced unipolar OFDM (eU-OFDM) [12], the enhanced pulse-amplitude-modulated discrete multitone modulation (ePAM-DMT) [13], and the augmented spectral efficiency discrete multitone (ASE-DMT) [14].

Besides communication, illumination is the other key feature of the practical VLC system [15], [16]. The VLC system is expected to provide high-speed communication under different required illumination levels. So far, several dimming control schemes have been proposed for conventional optical OFDM. In [17], an inverse source coding based method using on-off keying was proposed to realize dimming control. Moreover in [18], the authors explored a multiple pulse position modulation based dimming method by changing the number of

0733-8724 © 2019 IEEE. Personal use is permitted, but republication/redistribution requires IEEE permission.
See http://www.ieee.org/publications_standards/publications/rights/index.html for more information.

optical pulses within one symbol duration for the pulse width modulation system. For the DCO-OFDM system, the authors generated the signal of DCO-OFDM by introducing a piecewise function with variable slopes according to the required optical power in [19]. And for the layered ACO-OFDM system, a dimming method adjusting the polarities of different layers of ACO-OFDM were introduced in [20] and an adaptive dimming method was investigated in [21] to achieve wide dimming range in the layered ACO-OFDM system for different illumination requirements.

Recently, subcarrier index modulation (SIM) has been introduced into the VLC systems to convey information bits in a more energy-efficient way. SIM is an emerging modulation technique, which creates completely new dimensions for data transmission [22]. Hence it has attracted tremendous interests over the past few years [23]. Specifically, in SIM, the information bits are mapped not only on the conventional constellation domain, but also on the index domain of the OFDM subcarriers [24]. In [25], the concept of the enhanced SIM is proposed to avoid bit error propagation whilst retaining the energy efficiency of SIM. In [26], the basic system structure of the SIM aided VLC system is proposed and it is shown that the SIM aided OFDM achieves better error performance than the classical optical OFDM schemes. Moreover, a modulation scheme which incorporates the SIM and the Reed Solomon coding is proposed for VLC to improve the bit error rate performance in [27]. Recent works have also extended the concept of the index selection to the LED domain [28]. However, to the best of our knowledge, there lacks dimming control scheme intended for the SIM aided VLC system, which is one of the key problems in the implementation of practical SIM aided VLC.

In this paper, we propose a novel hybrid dimming scheme for the indoor SIM aided VLC system. In the proposed scheme, the frequency-domain and intensity-domain dimming strategies are merged to accommodate dimmable indoor communication. We analyze the channel capacity of the SIM aided VLC system and obtain the closed-form approximation of the channel capacity through mutual information analysis in both the line-of-sight (LOS) channel and the multipath channel. The frequency-domain optimization is realized based on the maximization of the channel capacity and then the intensity-domain dimming is achieved to further adjust the illumination level. Numerical simulations are carried out in both the LOS and the multipath channels and the results demonstrate the superior performance of the proposed scheme.

The rest of this paper is organized as follows. In Section II, the system model of the SIM based VLC and the indoor VLC channel model are explained in detail. In Section III, the channel capacity is analyzed and the SIM based frequency-intensity-domain hybrid dimming scheme is proposed in both the LOS channel and the multipah channel. Then the numerical simulations are carried out under both channel scenarios and the results are provided in Section IV. Finally, we conclude the paper in Section V.

Notation: $\binom{\cdot}{\cdot}$ denotes the binomial coefficient; $\delta(\cdot)$ denotes the Dirac delta function; factorial and derivative are denoted by $(\cdot)!$ and $(\cdot)'$, respectively.

II. System Model

A. SIM Aided VLC

We consider a SIM aided VLC system with ACO-OFDM, the system model is illustrated in Fig. 1. The bandwidth of the system is denoted as W, which is divided into N_{F} subcarriers. Without loss of generality, the ACO-OFDM is adopted as an example. Because the Hermitian symmetry needs to be satisfied and only the odd subcarriers are modulated in ACO-OFDM, only $N = N_{\mathrm{F}}/4$ subcarriers are available for index selection and independent data transmission.

Using SIM, the available subcarriers are split into G groups and each group consists of $L = N/G$ subcarriers. In each group, K out of L subcarriers are activated to transmit information. Thus, the input bits are first divided into G groups. Then in each group, $\lfloor \log_2 \binom{L}{K} \rfloor$ bits are used to select the activated subcarriers and the remaining bits are utilized to decide the M-ary phase shift keying (PSK) or quadrature amplitude modulation (QAM) modulated symbols at the activated subcarriers. For group g_i with $i \in \{1, 2, \ldots, G\}$, the set of selected subcarrier indices is given as

$$\Omega_{g_i} = \{\omega_1^{g_i}, \omega_2^{g_i}, \ldots, \omega_K^{g_i}\}, \tag{1}$$

where $\omega_k^{g_i} \in \{1, 2, \ldots, N\}$ and $k = 1, 2, \ldots, K$. According to the principle of SIM, $\Omega_{g_1} \cap \Omega_{g_2} = \varnothing$, with $g_1 \neq g_2$.

After the index selection, the OFDM block is created according to the selected subcarrier indices and mapped constellation symbols in all groups. Therefore the frequency-domain OFDM symbol $\mathbf{S}$ is given as

$$\mathbf{S} = [0, S_1, 0, S_3, \ldots, S_{N_{\mathrm{F}}/2-1}, 0, S^*_{N_{\mathrm{F}}/2-1}, \ldots, 0, S_1^*], \tag{2}$$

where S_k denotes the symbol transmitted at the k-th subcarrier, which is selected from the extended constellation set $\{0, \mathrm{QAM(PSK)}\}$. Then a N_{F}-point inverse fast Fourier transform (IFFT) is applied to obtain the time-domain samples,

$$s_n = \frac{1}{\sqrt{N_{\mathrm{F}}}} \sum_{k=1}^{N_{\mathrm{F}}} S_k e^{\frac{j2\pi nk}{N_{\mathrm{F}}}}. \tag{3}$$

Because of the utilization of only the odd numbered subcarriers in the frequency-domain ACO-OFDM symbols, the time-domain samples satisfy the anti-symmetry property, which is given as

$$s_n = -s_{n+(N_{\mathrm{F}}/2)}, 0 < n < \frac{N_{\mathrm{F}}}{2}. \tag{4}$$

Thus, either the positive part or the negative part of the time-domain samples can be clipped without any information loss. The positive and negative clipped time-domain samples are further given as

$$s_n^{\mathrm{PACO}} = \begin{cases} s_n, & s_n \geq 0, \\ 0, & s_n < 0, \end{cases} \tag{5}$$

and

$$s_n^{\mathrm{NACO}} = \begin{cases} 0, & s_n > 0, \\ s_n, & s_n \leq 0, \end{cases} \tag{6}$$

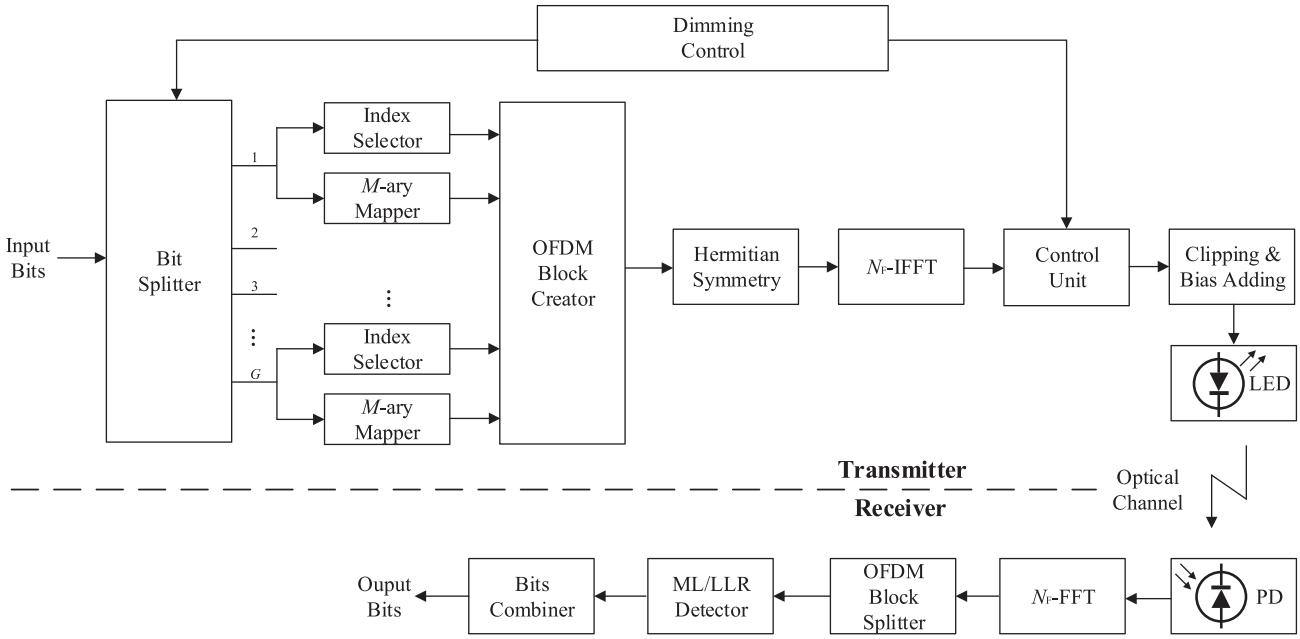


Fig. 1. The system model of the SIM based hybrid dimming scheme for VLC.

where s_n^{PACO} and s_n^{NACO} denote the positive and negative ACO-OFDM samples, respectively. Then the samples are rescaled and added to the direct current bias. The transmitted time-domain positive and negative ACO-OFDM samples are further given as

$$x_n^{\mathrm{PACO}} = \begin{cases} \beta s_n + I_{\mathrm{L}}, & 0 \le s_n \le (\frac{I_{\mathrm{H}} - I_{\mathrm{L}}}{\beta}), \\ I_{\mathrm{L}}, & s_n < 0, \end{cases} \tag{7}$$

and

$$x_n^{\mathrm{NACO}} = \begin{cases} I_{\mathrm{H}}, & s_n > 0, \\ \beta s_n + I_{\mathrm{H}}, & (\frac{I_{\mathrm{L}} - I_{\mathrm{H}}}{\beta}) \le s_n \le 0, \end{cases} \tag{8}$$

where β is the scaling factor. I_{L} and I_{H} denote the allowed minimum and maximum intensities of the dynamic range of the LEDs, respectively. Then the time-domain samples are transmitted over the optical channel.

At the receiver, the fast Fourier transform (FFT) is applied to obtain the frequency-domain signals. Then, the frequency-domain OFDM signals are split into G groups. In each group, the optimal maximum-likelihood (ML) detector can be used to decode the information bits. The log-likelihood ratio (LLR) detector can also be utilized to achieve a trade-off between the detection complexity and the detection accuracy. The detailed methods of these detectors can be found in [29]. Finally, the decoded bits in each group are combined to obtain the output bits. The frequency-domain transmission equation can be given as

$$Y_k = X_k H_k + W_k, k = 1, 2, \ldots, N_{\mathrm{F}}, \tag{9}$$

where X_k and Y_k denote the frequency-domain transmitted and received signals at the k-th subcarrier, respectively. H_k is the frequency-domain optical channel coefficient and $W_k \sim \mathcal{N}(0, \sigma^2)$ is the additive white Gaussian noise (AWGN) with variance σ^2.

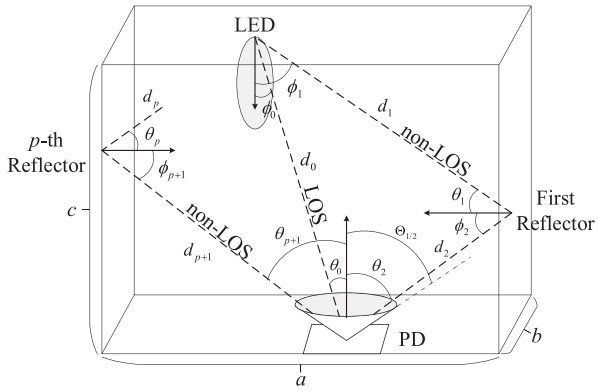


Fig. 2. The geometry of the indoor VLC channel.

B. Indoor Channel Characteristics for VLC

The indoor VLC scenario is considered in this paper and the widely used channel models proposed in [30] and [31] are adopted. We consider an empty cubic room with length a, width b, and height c, respectively. The LED is located on the ceiling of the room and the photo detector (PD) is placed on the floor. The optical signal can be transmitted by either the LOS path or the non-LOS paths, which are due to the reflections from the walls, ceilings and floors. The geometry of the indoor VLC channel is illustrated in Fig. 2.

1) Line-of-Sight Channel Characteristics: According to [30], the channel impulse response (CIR) of the LOS path can be approximated as a scaled and delayed Dirac delta function,

which is given as

$$h^{(0)}(t) = \frac{(m+1)A_{\mathrm{R}}}{2\pi d_0^2}\cos^m(\phi_0)\cos(\theta_0)\mathrm{rect} \times \left(\frac{\theta_0}{\Theta_{1/2}}\right)\delta\left(t - \frac{d_0}{c_{\mathrm{light}}}\right), \tag{10}$$

where ϕ_0, θ_0, and d_0 denote the angle of irradiance, the angle of incidence, and the distance between the LED and the PD in the LOS path, respectively. A_{R} and $\Theta_{1/2}$ denote the area and the semi-angle of the field of view (FOV), respectively. c_{light} is the speed of light. $\mathrm{rect}(x)$ denotes the rectangular function, which is given by

$$\mathrm{rect}(x) = \begin{cases} 1, & |x| \le 1, \\ 0, & |x| > 1. \end{cases} \tag{11}$$

The Lambertian mode number m can be further expressed as

$$m = -\frac{\ln 2}{\ln(\cos\Phi_{1/2})}, \tag{12}$$

where $\Phi_{1/2}$ denotes the half-intensity radiation angle of the LED. The Lambertian mode number specifies the directionality of the source. $m = 1$ corresponds to the traditional Lambertian source and larger Lambertian mode number implies higher directionality [32]. Thus, the channel DC gain is given by

$$H_{\mathrm{L}}(0) = \int_{-\infty}^{\infty} h^{(0)}(t) = \begin{cases} \frac{(m+1)A_{\mathrm{R}}}{2\pi d_0^2}\cos^m(\phi_0)\cos(\theta_0), & 0 \le \theta_0 \le \Theta_{1/2} \\ 0, & \text{elsewhere.} \end{cases} \tag{13}$$

The total noise power is given as $\sigma^2 N_{\mathrm{F}}$. Therefore, the signal to noise ratio (SNR) at the receiver is given as

$$\gamma_{\mathrm{L}} = \frac{\rho H_{\mathrm{L}}(0)^2 P}{\sigma^2 N_{\mathrm{F}}}, \tag{14}$$

where P is the total transmit electric power of the whole system. ρ denotes the overall effect of the optical-to-electrical, analog-to-digital, digital-to-analog, and electrical-to-optical domain coefficients, which is taken as unity in this paper.

2) Multipath Channel Characteristics: In the indoor VLC environments, the optical signals can also be received by the PD through the reflections from the walls and other objects, which causes multipath propagations. According to [33], experimental measurements have shown that many materials such as plaster, carpets and unvarnished wood can be seen as Lambertian reflectors. As a result, the multipath channel is approximated based on the diffusive ideal Lambertian assumption [31]. Thus, the CIR after p reflections is given as

$$h^{(p)}(t) = \int_S \left[M_1 M_2 \cdots M_{p+1}\mathrm{rect}\left(\frac{\theta_{p+1}}{\Theta_{1/2}}\right) \times \delta\left(t - \frac{d_1 + d_2 + \cdots + d_{p+1}}{c_{\mathrm{light}}}\right)\right] \cdot \mathrm{d}A_{\mathrm{ref}}, p \ge 1, \tag{15}$$

and $M_q (q = 1, 2, \ldots, p+1)$ are further given as

$$M_q = \begin{cases} \frac{A_{\mathrm{ref}}(m+1)\cos^m\phi_q\cos\theta_q}{2\pi d_q^2}, & q = 1, \\ \frac{A_{\mathrm{ref}}\cos\phi_q\cos\theta_q}{\pi d_q^2}, & 1 < q < p, \\ \frac{A_{\mathrm{R}}\cos\phi_q\cos\theta_q}{\pi d_q^2}, & q = p+1, \end{cases} \tag{16}$$

where ϕ_q, θ_q, and d_q denote the angle of irradiance, the angle of incidence, and the distance of the q-th reflection, respectively. A_{ref} denotes the area of the reflecting element. Therefore, the CIR of the multipath channel can be derived as

$$h(t) = \sum_{p=0}^{\infty} h^{(p)}(t). \tag{17}$$

Since the channel gain of LOS path is independent of the modulation frequency [34], the channel gain of the multipath channel at frequency f can be given as

$$H_{\mathrm{M}}(f) = H_{\mathrm{L}}(0) + \sum_{p=1}^{\infty} H_{\mathrm{D},p}(f), \tag{18}$$

where $H_{\mathrm{D,p}}(f)$ denotes the channel gain of the non-LOS diffuse link after p reflections at frequency f. Therefore, in the multipath channel, the SNR at the receiver is given as

$$\gamma_{\mathrm{M}}(f) = \frac{\rho H_{\mathrm{M}}(f)^2 P}{\sigma^2 N_{\mathrm{F}}}. \tag{19}$$

III. Proposed Hybrid Dimming Scheme

In this section, the SIM based hybrid dimming scheme is proposed based on the maximization of the channel capacity.

A. Channel Capacity Analysis

In each group of the SIM aided VLC system, the mutual information can be decomposed by using the chain rule of mutual information, which is not conditioned on whether the random variables are dependent or not,

$$I(\mathbf{x}_{\mathrm{s}}, \mathbf{x}_{\mathrm{c}}; \mathbf{y}) = I(\mathbf{x}_{\mathrm{s}}; \mathbf{y}|\mathbf{x}_{\mathrm{c}}) + I(\mathbf{x}_{\mathrm{c}}; \mathbf{y}), \tag{20}$$

where $\mathbf{x}_{\mathrm{c}}$ and $\mathbf{x}_{\mathrm{s}}$ denote the index-domain symbols and the constellation-domain symbols in each group, respectively. Thus, the total mutual information can be expressed as the sum of the index-domain information $I(\mathbf{x}_{\mathrm{c}}; \mathbf{y})$ and the constellation-domain information $I(\mathbf{x}_{\mathrm{s}}; \mathbf{y}|\mathbf{x}_{\mathrm{c}})$. We follow [35] to conduct the mutual information analysis.

According to the properties of the mutual information, the constellation-domain part can be given as

$$I(\mathbf{x}_{\mathrm{s}}; \mathbf{y}|\mathbf{x}_{\mathrm{c}}) = \sum_{j=1}^{\binom{L}{K}} \Pr(\mathbf{x}_{\mathrm{c}} = \Psi_j) I(\mathbf{x}_{\mathrm{s}}; \mathbf{y}|\mathbf{x}_{\mathrm{c}} = \Psi_j), \tag{21}$$

where Ψ_j denotes the j-th index-domain symbol with $j \in \{1, 2, \ldots, \binom{L}{K}\}$. Suppose the activated subcarriers are selected

with equal probability, which means $\Pr(\mathbf{x}_\mathrm{c} = \Psi_j) = 1/\binom{L}{K}$. Therefore, the mutual information can be further derived as

$$I(\mathbf{x}_\mathrm{s}; \mathbf{y}|\mathbf{x}_\mathrm{c}) = \frac{1}{\binom{L}{K}} \sum_{j=1}^{\binom{L}{K}} \sum_{i \in \Psi_j} \log_2 \left(1 + \frac{P}{2GK} \times \frac{H_i^2}{\sigma^2}\right) = \frac{K}{L} \sum_{i=1}^{L} \log_2 \left(1 + \frac{H_i^2 P}{2\sigma^2 GK}\right). \quad (22)$$

On the other hand, the index-domain mutual information can be given as

$$I(\mathbf{x}_\mathrm{c}; \mathbf{y}) = \frac{1}{\binom{L}{K}} \sum_{j=1}^{\binom{L}{K}} \int_{\mathbf{y}} f(\mathbf{y}|\mathbf{x}_c = \Psi_j) \times \log_2 \left(\frac{f(\mathbf{y}|\mathbf{x}_c = \Psi_j)}{f(\mathbf{y})}\right) \mathrm{d}\mathbf{y}, \quad (23)$$

where $f(\mathbf{y})$ is the probability distribution function of $\mathbf{y}$, and $f(\mathbf{y}|\mathbf{x}_c = \Psi_j)$ is the conditional probability distribution function when $\mathbf{x}_c = \Psi_j$. According to [36], the index-domain mutual information has no closed-form expression. Thus, the upper bound of the index-domain mutual information can be utilized as an approximation, which is given by

$$I(\mathbf{x}_\mathrm{c}; \mathbf{y}) \approx \log_2 \binom{L}{K}. \quad (24)$$

The channel capacity C of the system is expressed as

$$C = \frac{W}{N_\mathrm{F}} G I(\mathbf{x}_\mathrm{s}, \mathbf{x}_\mathrm{c}; \mathbf{y}) = \frac{W}{4L}(I(\mathbf{x}_\mathrm{s}; \mathbf{y}|\mathbf{x}_\mathrm{c}) + I(\mathbf{x}_\mathrm{c}; \mathbf{y})). \quad (25)$$

We substitute (22) and (24) into (25), and the approximation of the channel capacity is finally derived as

$$C \approx \frac{W}{4L} \left(\frac{K}{L} \sum_{i=1}^{L} \log_2 \left(1 + \frac{H_i^2 P}{2\sigma^2 GK}\right) + \log_2 \binom{L}{K}\right) \approx \frac{WK}{4L^2} \sum_{i=1}^{L} \log_2 \left(1 + \frac{H_i^2 P}{2\sigma^2 GK}\right) + \frac{W}{4L} \log_2 \binom{L}{K}. \quad (26)$$

B. SIM Based Frequency-Domain Optimization

The proposed hybrid dimming scheme consists of two steps. In the first step, the frequency-domain dimming is applied based on the maximization of the channel capacity. Since the channel capacity is related to the optical channel gain at different subcarriers, the frequency-domain optimization strategies in the LOS channel and the multipath channel are explained respectively.

1) LOS Channel scenario: The second part of (26) can be approximated using the Stirling's approximation, which is expressed as

$$\frac{W}{4L} \log_2 \binom{L}{K} = \frac{W}{4L} \log_2 \frac{L!}{K!(L-K)!} \approx \frac{W}{4L} \Bigg[\left(L + \frac{1}{2}\right) \log_2(L) - \left(L - K + \frac{1}{2}\right) \log_2(L-K) - \left(K + \frac{1}{2}\right) \log_2(K) - \frac{\log_2(2\pi)}{2} \Bigg]. \quad (27)$$

When the LOS channel is considered, the optical channel gain is independent of the frequency. Thus, the channel gains at different subcarriers are the same, which are

$$H_k = H_\mathrm{L}(0), k = 1, 2, \ldots, L. \quad (28)$$

As a result, the first part of (26) can be further simplified as

$$\frac{WK}{4L^2} \sum_{i=1}^{L} \log_2 \left(1 + \frac{H_i^2 P}{2\sigma^2 GK}\right) = \frac{WK}{4L^2} \sum_{i=1}^{L} \log_2 \left(1 + \frac{H_\mathrm{L}(0)^2 P}{2\sigma^2 GK}\right) = \frac{WK}{4L} \log_2 \left(1 + \frac{2\gamma L}{K}\right). \quad (29)$$

Thus, the channel capacity in the LOS channel is further approximated as

$$C \approx \frac{WK}{4L} \log_2 \left(1 + \frac{2\gamma L}{K}\right) + \frac{W}{4L} \Bigg[\left(L + \frac{1}{2}\right) \log_2(L) - \frac{\log_2(2\pi)}{2} - \left(L - K + \frac{1}{2}\right) \log_2(L-K) - \left(K + \frac{1}{2}\right) \log_2(K) \Bigg], \quad (30)$$

and the derivative of C in terms of K is given as

$$C' = \frac{W}{4L} \log_2 \left(\frac{(K + 2\gamma L)(L-K)}{K^2}\right) - \frac{W}{4 \ln 2L(K + 2\gamma L)} + \frac{W(2L - 2K + 1)}{8 \ln 2L(L-K)} - \frac{W(2K+1)}{8 \ln LK}. \quad (31)$$

In order to maximize the channel capacity, the optimal number of activated subcarriers in each group K can be derived by solving the equation $C' = 0$. The equation can be solved through many numerical iterative methods, including the steepest descent algorithm, the conjugate gradient method and so on.

2) Multipath Channel scenario: In the multipath channel, the non-LOS channels are taken into consideration due to the reflections from the walls and ceilings. As shown in Section II-B, the multipath channel gains are related to the modulation frequency, thus they are not the same at different subcarriers. The second part of (26) can also be approximated using the Stirling's approximation as shown in (27). As a result, the channel capacity

in the multipath channel can be approximated as

$$C \approx \frac{WK}{4L^2}\sum_{i=1}^{L}\log_2\left(1+\frac{H_i^2P}{2\sigma^2GK}\right) + \frac{W}{4L}\left[\left(L+\frac{1}{2}\right)\log_2(L) - \frac{\log_2(2\pi)}{2} - \left(L-K+\frac{1}{2}\right)\log_2(L-K) - \left(K+\frac{1}{2}\right)\log_2(K)\right]. \tag{32}$$

Thus, the optimal number of activated subcarriers in each group can be derived by calculating the derivative of C in terms of K, which is given as

$$C' = \frac{W}{4L^2}\sum_{i=1}^{L}\log_2\left(1+\frac{H_i^2P}{2\sigma^2GK}\right) - \frac{WK}{4L^2}\sum_{i=1}^{L}\frac{H_i^2P}{\ln 2K^2(2\sigma^2GK+H_i^2P)} - \frac{W}{4\ln 2L(K+2\gamma L)} + \frac{W(2L-2K+1)}{8\ln 2L(L-K)} - \frac{W(2K+1)}{8\ln LK}. \tag{33}$$

Since the closed-form solution of $C'=0$ is not easy to obtain, numerical iterative methods can be used to solve the equation.

C. ACO-OFDM Based Intensity-Domain Dimming

In the second step, the proportions of the positive and the negative ACO-OFDM symbols are further adjusted to meet the illumination requirements. The dimming level of the SIM aided VLC system can be described as

$$\eta = \frac{\mathbb{E}[I_{\mathrm{LED}}]-I_{\mathrm{L}}}{(I_{\mathrm{H}}-I_{\mathrm{L}})}\times 100\%, \tag{34}$$

where $\mathbb{E}[I_{\mathrm{LED}}]$ denotes the expectation of the LED intensity. As a result, according to (34), if a specific illumination level η is required, the expectation $\mathbb{E}[I_{\mathrm{LED}}]$ should be set to

$$\mathbb{E}[I_{\mathrm{LED}}] = \eta(I_{\mathrm{H}}-I_{\mathrm{L}})+I_{\mathrm{L}}. \tag{35}$$

According to [37], the ACO-OFDM symbols follow the clipped Gaussian distribution, the expectation of which is derived as $\sigma_{\mathrm{s}}/\sqrt{2\pi}$, where σ_{s} denotes the root mean square of the unclipped Gaussian distributed symbols. Thus, after the clipping process and the bias adding process, the expectations of the positive and negative ACO-OFDM symbols are given as

$$\mathbb{E}[I^{\mathrm{PACO}}] = I_{\mathrm{L}}+\frac{\sigma_{\mathrm{s}}}{\sqrt{2\pi}}, \tag{36}$$

and

$$\mathbb{E}[I^{\mathrm{NACO}}] = I_{\mathrm{H}}-\frac{\sigma_{\mathrm{s}}}{\sqrt{2\pi}}, \tag{37}$$

where $\mathbb{E}[I^{\mathrm{PACO}}]$ and $\mathbb{E}[I^{\mathrm{NACO}}]$ denote the expectation of the positive and negative ACO-OFDM symbols, respectively. Thus, the proportion of the two kinds of symbols can be utilized to adjust the expectation of the LED intensity. If we denote the proportion of the positive ACO-OFDM symbols as α, the expectation of LED intensity can be expressed as

$$\mathbb{E}[I_{\mathrm{LED}}] = \alpha(I_{\mathrm{L}}+\frac{\sigma_{\mathrm{s}}}{\sqrt{2\pi}})+(1-\alpha)(I_{\mathrm{H}}-\frac{\sigma_{\mathrm{s}}}{\sqrt{2\pi}}). \tag{38}$$

Combining (35) and (38), the proportion α is derived according to the given illumination level, which is

$$\alpha = \begin{cases} 1, & \eta < \eta_{\min}, \\ \dfrac{(\eta-1)(I_{\mathrm{H}}-I_{\mathrm{L}})+\sigma_{\mathrm{s}}/\sqrt{2\pi}}{I_{\mathrm{L}}-I_{\mathrm{H}}+2\sigma_{\mathrm{s}}/\sqrt{2\pi}}, & \eta_{\min}\le\eta\le\eta_{\max}, \\ 0, & \eta > \eta_{\max}, \end{cases} \tag{39}$$

where $\eta_{\min}$ and $\eta_{\max}$ are given as

$$\eta_{\min} = \frac{\sigma_{\mathrm{s}}}{(I_{\mathrm{H}}-I_{\mathrm{L}})\sqrt{2\pi}}, \tag{40}$$

and

$$\eta_{\max} = 1-\frac{\sigma_{\mathrm{s}}}{(I_{\mathrm{H}}-I_{\mathrm{L}})\sqrt{2\pi}}. \tag{41}$$

As a result, under the appropriate illumination level $\eta_{\min}<\eta<\eta_{\max}$, both the positive and negative ACO-OFDM symbols are transmitted with the proportion α.

If the illumination requirement is higher than $\eta_{\max}$ or lower than $\eta_{\min}$, only the negative or the positive symbols are utilized. In conventional dimming schemes, the scaling factor is further adjusted to meet the illumination requirement. While in our proposed hybrid dimming scheme, the number of activated subcarriers K provides another dimension for dimming control. Specifically, under the specific illumination levels $\eta_1>\eta_{\max}$ and $\eta_2<\eta_{\min}$, the transmitted symbols are required as

$$\sigma_{\mathrm{s},1} = \sqrt{2\pi}(1-\eta_1)(I_{\mathrm{H}}-I_{\mathrm{L}}), \tag{42}$$

and

$$\sigma_{\mathrm{s},2} = \sqrt{2\pi}\eta_2(I_{\mathrm{H}}-I_{\mathrm{L}}). \tag{43}$$

Therefore, the total transmit electric power can be further given as

$$P_1 = \frac{GK\sigma_{\mathrm{s},1}^2}{2} = \pi GK(1-\eta_1)^2(I_{\mathrm{H}}-I_{\mathrm{L}})^2, \tag{44}$$

and

$$P_2 = \frac{GK\sigma_{\mathrm{s},2}^2}{2} = \pi GK\eta_2^2(I_{\mathrm{H}}-I_{\mathrm{L}})^2. \tag{45}$$

Thus, the optimal K can be derived by substituting (44) and (45) into (30) and (32) to maximize the channel capacity in the LOS channel and the multipath channel, respectively. As a result, the required illumination level is achieved from both the frequency- and intensity-domain dimming methods.

The proposed hybrid dimming scheme can also be extended to other sophisticated optical waveforms such as layered ACO-OFDM [8] and eU-OFDM [12]. In these layered OFDM schemes, the proposed positive and negative symbols with different expected intensities can be transmitted on each layer to

TABLE I
PARAMETERS FOR SIMULATION

Parameter	Explication	Value
N_{F}	Number of subcarriers	256
N	Number of subcarriers for index selection	64
G	Number of subcarrier groups	4
I_{L}	Minimum intensity level of the LED	0 A
I_{H}	Maximum intensity level of the LED	1 A
m	Lambertian mode number of the LED	1
A_{R}	Area of the PD	1 cm^2
$\Theta_{1/2}$	Semi-angle of the FOV of the PD	85°
W	System bandwidth	4 MHz

provide dimming control. The channel capacity can also be optimized through the proposed frequency-domain optimization procedure.

IV. SIMULATION RESULTS

In this section, the simulation results are provided to show the performance of the proposed hybrid dimming scheme. We consider a SIM aided VLC system in an empty cubic room with length $a = 5.0$ m, width $b = 5.0$ m, and height $c = 3.0$ m. An LED is located on the center of the ceiling (2.5 m, 2.5 m, 3.0 m) pointing straight down and a PD is placed on the corner of the floor (0.5 m, 1.0 m, 0 m) pointing straight up. The ACO-OFDM and eU-OFDM are adopted to show the performance, respectively. The simulations are carried out in both the LOS channel and the multipath channel. The simulation parameters are summarized in Table I.

In the multipath channel, the first three non-LOS paths are taken into consideration. The multipath channel parameters given in [30] are used in the simulation, where the channel gain of the LOS path is 1.232×10^{-6} and the channel gain of the first three non-LOS paths are 0.467×10^{-6}, 0.211×10^{-6}, and 0.107×10^{-6}, respectively. The channel frequency response (CFR) can be derived by applying the Fourier transform to the CIR. The CIR and the CFR of the multipath channel are illustrated in Fig. 3.

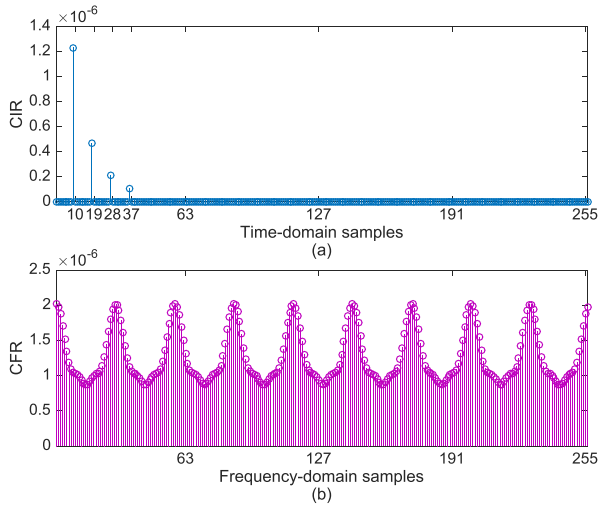


Fig. 3. Illustration of the CIR and the CFR in the multipath channel. (a) The CIR of the multipath channel. (b) The amplitude of the CFR.

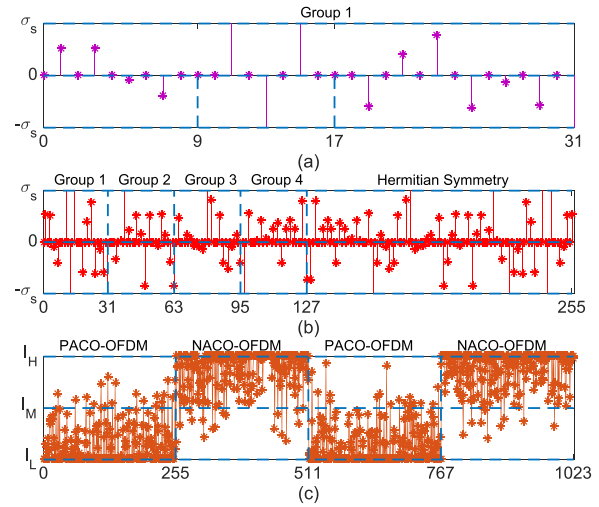


Fig. 4. Illustration of the transmitted samples in both the frequency domain and the time domain. (a) The real part of the frequency-domain samples in the first group. (b) The real part of the samples in one frequency-domain symbol. (c) The samples in four time-domain symbols.

The illustrations of the transmitted frequency-domain and time-domain samples are given in Fig. 4 with $\gamma = 10$ dB and $K = 14$. Fig. 4(a) shows the real part of the transmitted frequency-domain samples in the first group. It can be seen that the information bits are only mapped on the odd subcarriers. Thus, $L = 16$ out of 32 subcarriers can be selected to transmit information. Since SIM is utilized, only $K = 14$ subcarriers are activated. It can be seen that in the illustration, the 9-th and the 17-th subcarriers are selected to be unactivated. Fig. 4(b) illustrates the real part of the whole frequency-domain symbol which contains $G = 4$ groups. The second half of the symbol is generated according to the Hermitian symmetry property as given in (2). Fig. 4(c) shows the corresponding time-domain samples. Since the illumination requirement is $\eta = 50\%$, the proportion of the positive ACO-OFDM symbols is $\alpha = 0.5$, which means half of the transmitted time-domain symbols are positive and the other half are negative ACO-OFDMs.

The closeness of the proposed approximation of the channel capacity is investigated in Fig. 5. In the simulation, we consider a SIM aided VLC system using ACO-OFDM in the LOS channel. The true values of the channel capacities are represented by the solid lines. The proposed closed-form approximations in (26) are depicted by the dotted lines. It can be seen from the figure that the proposed closed-form approximations can track the trends of the true values very well and are very close to the true values, which validates the effectiveness of the proposed closed-form approximations. It can be seen that the approximations are closer to the true values with higher SNRs. For instance, the average gap between the true value and the approximation is 0.0464 bits/s/Hz when SNR $= 12$ dB, while it becomes 0.0050 bits/s/Hz when

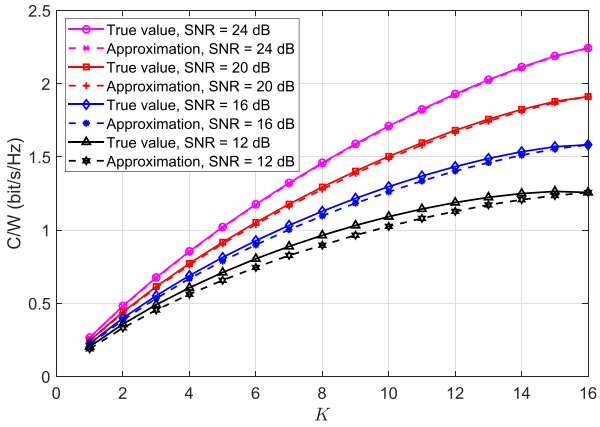


Fig. 5. Comparisons of the true values and the approximations of the channel capacities with different numbers of activated subcarriers K.

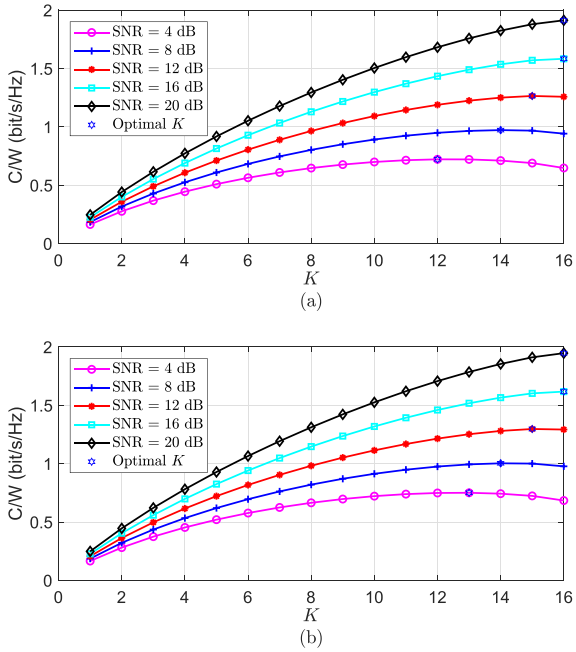


Fig. 6. Channel capacity versus the number of activated subcarriers in each group, where the number of subcarriers in each group is $L = 16$. (a) The LOS channel scenario. (b) The multipath channel scenario.

SNR $= 24$ dB. It can also be seen that the approximations are closer to the true values with a smaller or larger number of activated subcarriers K, which is mainly because the index-domain mutual information decreases with a smaller or larger number of K. For example, when SNR $= 20$ dB, the gap between the true value and the approximation is 0.0153 bits/s/Hz with $K = 8$, however, it becomes 0.0039 bits/s/Hz and 0.0085 bits/s/Hz when $K = 1$ and $K = 15$, respectively.

In Fig. 6, the channel capacities with different numbers of activated subcarriers and SNRs are investigated in both the LOS channel and the multipath channel. It can be seen from the figure that with the same number of activated subcarriers, the channel capacity rises with the increase of the SNR, which is mainly because of the improvement of the constellation-domain

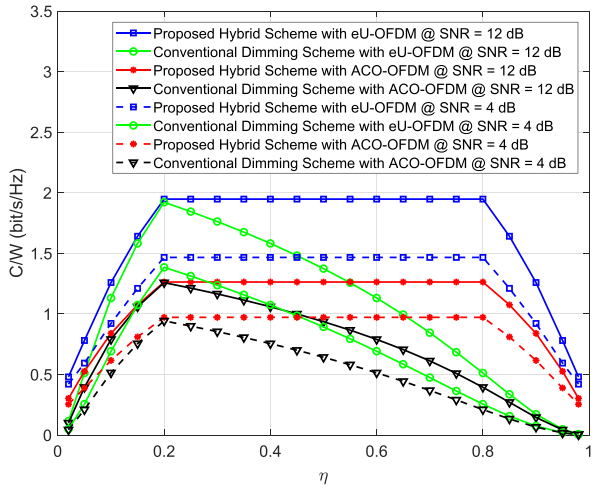


Fig. 7. Comparison of the channel capacity versus the illumination levels η in the LOS channel, where the number of subcarriers in each group is $L = 16$.

capacity with higher SNR. It can also be seen that the optimal number of activated subcarriers is different with different SNRs. For example, in the LOS channel as shown in Fig. 6(a), the optimal number is $K = 14$ with SNR $= 8$ dB and $K = 15$ with SNR $= 12$ dB. It is worth noting that the optimal number of activated subcarriers becomes larger with higher SNR. It is because that under the lower SNR situation, the contribution of the constellation-domain capacity to the total channel capacity is limited. Therefore, a smaller number of activated subcarriers can provide the larger index-domain capacity to maximize the total channel capacity. While under the higher SNR situation, the constellation-domain capacity improves and dominates the total channel capacity. Thus, more subcarriers are activated to realize the maximization of the total channel capacity. It can also be seen that under the same configuration, the channel capacities in the multipath channel are higher than those in the LOS channel, which is because the non-LOS paths can provide approaches for data transmission as well. However, the performance gap is not so large. It is because in the simulation, only three non-LOS paths are considered, and the channel gains of the non-LOS paths are much smaller than the LOS path. The total channel gain is dominated by the LOS path. Moreover, uniform power allocation is adopted in the simulation. Since the CFRs of the subcarriers are different in the multi-path channel scenario, power allocation strategies can be applied to further improve the channel capacity.

In Fig. 7, the channel capacities with different illumination requirements and different optical OFDM schemes are investigated in the LOS channel. The conventional dimming scheme using scaling factor and bias adjustments is also simulated as comparisons. The root mean square of the unclipped Gaussian distributed symbols is limited as $\sigma_s \leq 0.5$. It can be seen from the figure that the proposed hybrid dimming scheme enjoys much higher channel capacity than the conventional dimming scheme especially under the appropriate and high illumination requirements. It is because that the illumination level can be controlled by the proportion of the positive and negative OFDM symbols in the proposed scheme while maintaining the channel capacity under appropriate illumination requirements. For

example, with ACO-OFDM, the proposed hybrid dimming scheme has 1.30 dB and 2.65 dB gains over the conventional dimming scheme when SNR $= 12$ dB and SNR $= 4$ dB under the illumination requirement $\eta = 50\%$. The performance gap becomes larger at high SNR region. For example, the gains become 5.06 dB and 8.65 dB, respectively, when the illumination requirement is $\eta = 80\%$. It can also be seen that with the same configurations, the eU-OFDM based scheme has much higher channel capacity than the ACO-OFDM based scheme, which shows the benefits of the multi-layer transmission in eU-OFDM. However, the proportion of the positive and negative OFDM symbols need to be calculated to control the illumination level, which involves extra computation complexity. It can also be seen that the proposed hybrid scheme enjoys higher channel capacity under the low dimming requirements, which is mainly because of the frequency-domain optimization step in the hybrid scheme. The adjustment of the number of the activated subcarriers provides another dimension for the channel capacity maximization.

V. Conclusion

In this paper, a novel spectral-efficient hybrid dimming scheme has been proposed for the indoor VLC system. The channel capacities in both the LOS channel and the multipath channel have been analyzed and the jointly frequency-intensity-domain dimming scheme has been proposed under both scenarios. Simulations are conducted in the LOS channel as well as the multipath channel. The results have validated the superior spectral efficiency of the proposed scheme under the whole range of dimming requirements over the state-of-the-art dimming schemes. In our future researches, more efforts will be devoted to the joint optimization and allocation of the multi-dimensional resources to achieve trade-offs between the communication and illumination performance, which will be the building blocks of the dimmable indoor and outdoor high-speed VLC, indoor VLC localization and smart homes.

References

[1] Z. Ghassemlooy, S. Arnon, M. Uysal, Z. Xu, and J. Cheng, "Emerging optical wireless communications-advances and challenges," *IEEE J. Sel. Areas Commun.*, vol. 33, no. 9, pp. 1738–1749, Sep. 2015.

[2] I. Stefan, H. Burchardt, and H. Haas, "Area spectral efficiency performance comparison between VLC and RF femtocell networks," in *Proc. IEEE Int. Conf. Commun.*, Budapest, Hungary, Jun. 2013, pp. 3825–3829.

[3] J. Armstrong, "OFDM for optical communications," *J. Lightw. Technol.*, vol. 27, no. 3, pp. 189–204, Feb. 2009.

[4] J. B. Carruthers and J. M. Kahn, "Multiple-subcarrier modulation for non-directed wireless infrared communication," *IEEE J. Sel. Areas Commun.*, vol. 14, no. 3, pp. 538–546, Apr. 1996.

[5] J. Armstrong and A. J. Lowery, "Power efficient optical OFDM," *Electron. Lett.*, vol. 42, no. 6, pp. 370–372, Mar. 2006.

[6] Y. Sun, F. Yang, and J. Gao, "Comparison of hybrid optical modulation schemes for visible light communication," *IEEE Photon. J.*, vol. 9, no. 3, pp. 1–13, Jun. 2017.

[7] S. D. Dissanayake and J. Armstrong, "Comparison of ACO-OFDM, DCO-OFDM and ADO-OFDM in IM/DD systems," *J. Lightw. Technol.*, vol. 31, no. 7, pp. 1063–1072, Apr. 2013.

[8] Q. Wang, C. Qian, X. Guo, Z. Wang, D. G. Cunningham, and I. H. White, "Layered ACO-OFDM for intensity-modulated direct-detection optical wireless transmission," *Opt. Express*, vol. 23, no. 9, pp. 12382–12393, May 2015.

[9] H. Elgala and T. D. C. Little, "SEE-OFDM: Spectral and energy efficient OFDM for optical IM/DD systems," in *Proc. IEEE 25th Annu. Int. Symp. Pers., Indoor, Mobile Radio Commun.*, Washington, DC, USA, Sep. 2014, pp. 851–855.

[10] M. S. Islim, D. Tsonev, and H. Haas, "On the superposition modulation for OFDM-based optical wireless communication," in *Proc. IEEE Global Conf. Signal Inf. Process.*, Orlando, FL, USA, Dec. 2015, pp. 1022–1026.

[11] A. J. Lowery, "Enhanced asymmetrically-clipped optical OFDM," *Opt. Express*, vol. 24, no. 1, pp. 3950–3966, Mar. 2016.

[12] D. Tsonev, S. Videv, and H. Haas, "Unlocking spectral efficiency in intensity modulation and direct detection systems," *IEEE J. Sel. Areas Commun.*, vol. 33, no. 9, pp. 1758–1770, Sep. 2015.

[13] M. S. Islim, D. Tsonev, and H. Haas, "Spectrally enhanced PAM-DMT for IM/DD optical wireless communications," in *Proc. IEEE 26th Annu. Int. Symp. Pers., Indoor, Mobile Radio Commun.*, Hong Kong, China, Aug. 2015, pp. 877–882.

[14] M. S. Islim and H. Haas, "Augmenting the spectral efficiency of enhanced PAM-DMT-based optical wireless communications," *Opt. Express*, vol. 24, no. 11, pp. 11 932–11 949, May 2016.

[15] A. Tsiatmas, C. P. M. J. Baggen, F. M. J. Willems, J. M. G. Linnartz, and J. W. M. Bergmans, "An illumination perspective on visible light communications," *IEEE Commun. Mag.*, vol. 52, no. 7, pp. 64–71, Jul. 2014.

[16] S. H. Lee, S. Jung, and J. K. Kwon, "Modulation and coding for dimmable visible light communication," *IEEE Commun. Mag.*, vol. 53, no. 2, pp. 136–143, Feb. 2015.

[17] J. K. Kwon, "Inverse source coding for dimming in visible light communications using NRZ-OOK on reliable links," *IEEE Photon. Technol. Lett.*, vol. 22, no. 19, pp. 1455–1457, Oct. 2010.

[18] K. Lee and H. Park, "Modulations for visible light communications with dimming control," *IEEE Photon. Technol. Lett.*, vol. 23, no. 16, pp. 1136–1138, Aug. 2011.

[19] Y. Yang, Z. Zeng, J. Cheng, and C. Guo, "An enhanced DCO-OFDM scheme for dimming control in visible light communication systems," *IEEE Photon. J.*, vol. 8, no. 3, pp. 1–13, Jun. 2016.

[20] Q. Wang, Z. Wang, L. Dai, and J. Quan, "Dimmable visible light communications based on multilayer ACO-OFDM," *IEEE Photon. J.*, vol. 8, no. 3, pp. 1–11, Jun. 2016.

[21] F. Yang, Y. Sun, and J. Gao, "Adaptive LACO-OFDM with variable layer for visible light communication," *IEEE Photon. J.*, vol. 9, no. 6, Dec. 2017, Art. no. 7907908.

[22] R. Abu-alhiga and H. Haas, "Subcarrier-index modulation OFDM," in *Proc. IEEE 20th Int. Symp. Pers., Indoor, Mobile Radio Commun.*, Tokyo, Japan, Sep. 2009, pp. 177–181.

[23] E. Basar, M. Wen, R. Mesleh, M. D. Renzo, Y. Xiao, and H. Haas, "Index modulation techniques for next-generation wireless networks," *IEEE Access*, vol. 5, pp. 16693–16746, 2017.

[24] E. Basar, "Index modulation techniques for 5G wireless networks," *IEEE Commun. Mag.*, vol. 54, no. 7, pp. 168–175, Jul. 2016.

[25] D. Tsonev, S. Sinanovic, and H. Haas, "Enhanced subcarrier index modulation (SIM) OFDM," in *Proc. IEEE GLOBECOM Workshops*, Houston, TX, USA, Dec. 2011, pp. 728–732.

[26] E. Basar and E. Panayirci, "Optical OFDM with index modulation for visible light communications," in *Proc. 4th Int. Workshop Opt. Wireless Commun.*, Istanbul, Turkey, Sep. 2015, pp. 11–15.

[27] N. Taherkhani and K. Kiasaleh, "Subcarrier-index modulation for Reed Solomon encoded OFDM-based visible light communication," in *Proc. 16th IEEE Annu. Consum. Commun. Netw. Conf.*, Las Vegas, NV, USA, Jan. 2019, pp. 1–4.

[28] A. Yesilkaya, E. Basar, F. Miramirkhani, E. Panayirci, M. Uysal, and H. Haas, "Optical MIMO-OFDM with generalized LED index modulation," *IEEE Trans. Commun.*, vol. 65, no. 8, pp. 3429–3441, Aug. 2017.

[29] E. Basar, U. Aygolu, E. Panayirci, and H. V. Poor, "Orthogonal frequency division multiplexing with index modulation," *IEEE Trans. Signal Process.*, vol. 61, no. 22, pp. 5536–5549, Nov. 2013.

[30] K. Lee, H. Park, and J. R. Barry, "Indoor channel characteristics for visible light communications," *IEEE Commun. Lett.*, vol. 15, no. 2, pp. 217–219, Feb. 2011.

[31] J. R. Barry, J. M. Kahn, W. J. Krause, E. A. Lee, and D. G. Messerschmitt, "Simulation of multipath impulse response for indoor wireless optical channels," *IEEE J. Sel. Areas Commun.*, vol. 11, no. 3, pp. 367–379, Apr. 1993.

[32] F. Miramirkhani and M. Uysal, "Channel modeling and characterization for visible light communications," *IEEE Photon. J.*, vol. 7, no. 6, pp. 1–16, Dec. 2015.

[33] J. M. Kahn, W. J. Krause, and J. B. Carruthers, "Experimental characterization of non-directed indoor infrared channels," *IEEE Trans. Commun.*, vol. 43, no. 234, pp. 1613–1623, Apr. 1995.
[34] Z. Ghassemlooy, W. Popoola, and S. Rajbhandari, *Optical Wireless Communications: System and Channel Modelling with MATLAB*. New York, NY, USA: Taylor & Francis, 2012.
[35] A. Younis and R. Mesleh, "Information-theoretic treatment of space modulation MIMO systems," *IEEE Trans. Veh. Technol.*, vol. 67, no. 8, pp. 6960–6969, Aug. 2018.
[36] M. Wen, X. Cheng, M. Ma, B. Jiao, and H. V. Poor, "On the achievable rate of OFDM with index modulation," *IEEE Trans. Signal Process.*, vol. 64, no. 8, pp. 1919–1932, Apr. 2016.
[37] F. Yang and J. Gao, "Dimming control scheme with high power and spectrum efficiency for visible light communications," *IEEE Photon. J.*, vol. 9, no. 1, pp. 1–12, Feb. 2017.

Tengjiao Wang received the B.S. degree from the Department of Electronic Engineering, Tsinghua University, Beijing, China, in 2016. He is currently working toward the Ph.D. degree with the DTV Technology Research and Development Center, Department of Electronic Engineering, Tsinghua University. His research interests lie in the field of visible light communications, wireless communications, multiple-input multiple-output systems, non-orthogonal multiple access, and sparse signal processing theory. He received the National Scholarship in 2018.

Fang Yang received the B.S.E. and Ph.D. degrees in electronic engineering from Tsinghua University, Beijing, China, in 2005 and 2009, respectively. He is currently an Associate Professor with the Research Institute of Information Technology, Tsinghua University. He has authored or coauthored more than 120 peer-reviewed journal and conference papers. He holds more than 40 Chinese patents and 2 PCT patents. His research interests lie in the fields of channel coding, channel estimation, interference cancellation, and signal processing techniques for communication system, especially in power line communication, visible light communication, and digital television terrestrial broadcasting. Dr. Yang received the IEEE Scott Helt Memorial Award (best paper award in IEEE Transactions in Broadcasting) in 2015. He is the Secretary General of Sub-Committee 25 of the China National Information Technology Standardization (SAC/TC28/SC25).

Changyong Pan received the B.Eng and M.Eng. degrees in electrical engineering from Tsinghua University, Beijing, China, in 1996 and 1998, respectively and worked for the same university upon his graduation. He is a Full Professor with the Research Institute of Information Technology, Tsinghua University. He has authored or coauthored more than 180 technical papers and published 8 technical books. He holds 34 patents, won national technical award three times and is also the winner of numerous other awards. He is Fellow of both IET and CIE.

Ling Cheng received the B.Eng. degree in electronics and information (cum laude) from Huazhong University of Science and Technology (HUST), Wuhan, China, in 1995, the M.Ing. degree (cum laude) and the D.Ing. degree in 2005 and 2011 both in electrical and electronics from the University of Johannesburg (UJ), Johannesburg, South Africa. In 2010, he joined University of the Witwatersrand (Wits) where he was promoted to Full Professor in 2019. He has served as the Vice-Chair of IEEE South African Information Theory Chapter since 2018. He has been a Visiting Professor with five universities and the Principal Advisor for more than 40 full research postgraduate students. His research interests are in telecommunications and artificial intelligence. He has authored or coauthored more than 90 research papers in journals and conference proceedings. He was awarded the Chancellor's medal in 2005, 2019, the National Research Foundation rating in 2014, and the IEEE ISPLC 2015 best student paper award to his Ph.D. student in Austin.

Jian Song received the B.Eng and Ph.D. degrees in electrical engineering from Tsinghua University, Beijing, China, in 1990 and 1995, respectively and worked for the same university upon his graduation. He has worked with The Chinese University of Hong Kong and University of Waterloo, Canada, in 1996 and 1997, respectively. He has been with Hughes Network Systems in USA for seven years before joining the faculty team in Tsinghua in 2005 as a Professor. He is currently the Director of Tsinghua's DTV Technology R&D center. He has been working in quite different areas of fiber-optic, satellite and wireless communications, as well as the power line communications. His current research interest is in the area of digital TV broadcasting. Dr. Song has authored or coauthored more than 200 peer-reviewed journal and conference papers. He holds 2 US and more than 40 Chinese patents. He is a fellow of IET.